JOURNAL OF MATERIALS SCIENCE **35** (2000) 4337–4341

Effect of oxidation treatment on Li capacity in disordered carbons - The surfing cards model

Y. SOREK*, P. ZHOU, J. E. FISCHER
Department of Materials Science and Engineering and the Laboratory for Research on the Structure of Matter, University of Pennsylvania, Philadelphia, PA 19104-6272, USA
E-mail: sorek@iibr.gov.il

T. ISHIHARA
Mitsubishi Chemical Company, Yokohama Research Center, Aoba-ku, Yokohama 227, Japan

Small angle neutron scattering and X-ray diffraction were used to study the effect of oxidation treatment on the structure and Li capacity of disordered carbons. The oxidation treatment increase the pore density and reduce the degree of parallel arrangement of graphene layers, all with no detectable change in pore size. Scattering from Li-doped samples indicates that the Lithium is most likely coating the pore surfaces rather than creating clusters inside the pores. The results are analyzed in terms of the newly proposed "potato-chips" (edge-connected graphene fragments, or "cards") model of amorphous carbons, from which we infer translation, or "surfing", of connected fragments during heat treatment.

1. Introduction

Disordered carbons are gaining attention as replacements for graphite in Li-ion batteries due to their high reversible Li capacities. A large variety of carbons prepared from various starting materials and treated at different temperatures were tested, and some exhibit specific Li-capacities three times greater than graphite [1]. Hard carbons contain mono-disperse micro-pores on the order of 1 nm diameter, as a result of randomly oriented graphene fragments with similar lateral dimensions [1]. These cavities are large enough to allow Li cluster formation, and therefore could contribute to anode capacity. In this work we studied the correlation between the amorphous carbon structure and Li capacity using small angle neutron scattering and X-ray diffraction. We chose small angle neutron scattering (SANS) to study the structural factors affecting the Li capacity, since this technique provides information about the size and roughness of internal scattering surfaces in heterogeneous media. The correlation between morphological characteristics and Li capacity was studied in carbon black by K. Takei *et al.* [2]. They found that irreversible Li capacity increased with BET surface area, most likely due to surface-electrolyte inter-phase (SEI) layer formation. However, the reversible capacity was found to be independent of BET surface area. The present work is motivated by the observation that an oxidation treatment was shown to increase Li capacity in "amorphous" carbon prepared from carbon-tar pitch. The purpose if this work is to correlate this improvement to structural factors, in particular the formation of pores in the carbon by the oxidation process.

2. Experimental details

SANS experiments were performed on Li-doped and pristine "amorphous" carbons produced from coal tar pitch. This material also contains substantial hydrogen as a result of low temperature treatment. Three carbon samples were tested: EB1 which contains 8 mol% H, EA1, an oxidation product of the same raw material, containing only 4 mol% H after processing. To obtain the oxidized carbon EA1, the coal pitch was oxidized in air and then heat treated at 1100°C in inert atmosphere for 3 hours. The non-oxidized sample (EB1) was derived from the same pitch, heat treated in the same way but without the oxidizing step. In addition, an amorphous carbon prepared from Epoxi-Novolac Resin (ENR) pyrolysed to 1000°C, this sample contains 4 mol% H. The surface areas determined by N_2 adsorption at 77 K are 1.7 m^2/g and 1.2–4.0 m^2/g for EB1 and EA1, respectively.

Solid state ^{13}C NMR measurements showed that the carbons are 100% Sp^2 hybridized. Previous electrochemical testing revealed the reversible Li capacities of 351 mAh/g and 267 mAh/g for EA1 and EB1 respectively.

SANS profiles of pristine and Li-doped EB1 and EA1 were taken using the 30 meter diffractometer (NG3) at the National Institute of Standards and Technology (NIST) [3]. The neutron wavelength was 5 Å and the sample-detector distances used were 1.5, 7.5 and 13 meters to cover the Q range 0.003–0.4 $Å^{-1}$ where $Q = 4\pi \sin\theta/\lambda$.

The Li doing of EA1 and EB1 was carried out electrochemically using 1 molar $LiPF_6$ in EC/DMC (1 : 1

* *Present Address*: Department of Environmental Physics, Life Science Research Israel, P.O. Box 19, 74100 Ness-Ziona, Israel.

by volume). The SANS data were corrected for background and empty-cell scattering, circularly averaged and converted to absolute intensity using standard scattering samples. Wide-angle X-ray diffraction was performed in Debye-Scherrer geometry using 1 mm capillaries, Cu K_α radiation and a 1-D position-sensitive detector.

3. Results

3.1. Effect of oxidation treatment

Fig. 1 shows the overall SANS spectra for EA1 and EB1. Several features are immediately apparent. First, the intensity above 0.05 $Å^{-1}$ is much greater for the oxidized sample EA1 (squares) than for its non-oxidized precursor EB1 (diamonds), consistent with the notion that oxidation increases porosity. second, Li doping of EA1 reduces the SANS intensity (line), which as discussed below argues against pore filling by Li clusters. Finally, for all samples it is possible to divide the scattering into two distinct Q regions. At very low Q, below 0.05 $Å^{-1}$, the scattering is from the interface between macroscopic carbon particles or grains and the surrounding vacuum, the characteristic length scale being at least 100's of Å. At higher Q we find a transition to a much smaller $I(Q)$ slope, characteristic of scattering from density inhomogeneity within a particle, i.e. pores. At low Q the normalized SANS intensity per unit mass of oxidized EA1 is similar to that from non-oxidized EB1, consistent with macroscopic observations which show no difference in particle size.

For the present purposes, the most important difference between EB1 and EA1 carbons lies in the Q region 0.4–0.05 $Å^{-1}$, Fig. 1. Both samples exhibit deviations from power law behavior, while the oxidized EA1 carbon shows higher scattering.

In the Q region above 0.2 $Å^{-1}$ where a plateau is observed, it is possible to fit $I(Q)$ to the Guinier approximation [4]:

$$I(Q) = I(0)\exp\left(\frac{-Q^2R_g^2}{3}\right), \qquad (1)$$

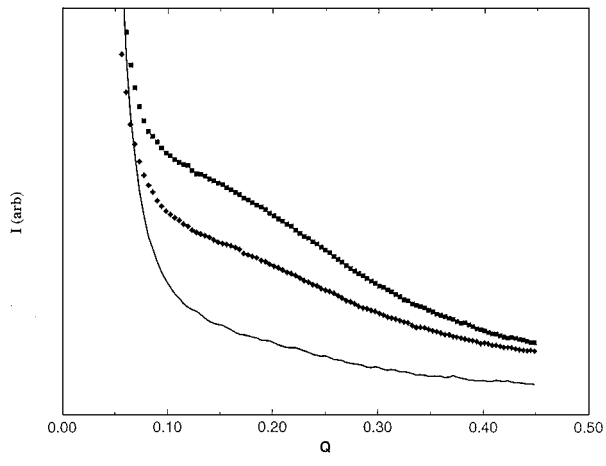

Figure 1 Linear plots of SANS intensity at low Q. Squares and solid line are for EA1 before and after Li doping respectively; diamonds are for pristine EB1 (the non-oxidized carbon).

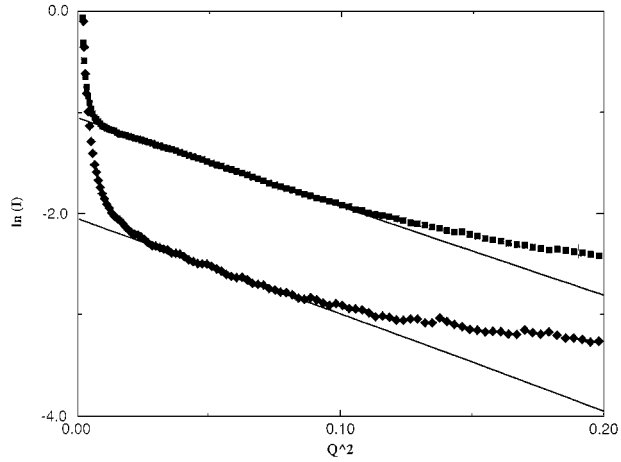

Figure 2 Guinier plots of EA1 (squares) and EB1 (diamonds). Solid lines are linear fits.

where R_g is the radius of gyration of the scattering structure.

The Guinier plots (Ln(I) vs. Q^2) are shown in Fig. 2, from which we deduce $R_g \sim 5$ Å. Extrapolating the Guinier plot to $Q = 0$ gives an estimate of $I(0)$ relevant to these scatterers: where n is the number of pores/volume, $\Delta\rho$ is the difference in neutron scattering length density across the pore surface (e.g. carbon vs. vacuum in pristine sample) and V_p is the volume of a pore. Assuming spherical pores with the above value of R_g, and using the scattering length density calculated from a contrast variation measurement (see below), we thus obtained the volume density of pores. We were unable to measure $\Delta\rho$ in a Q range corresponding to the Guinier behavior since a large fraction of the pores are isolated and thus inaccessible to the different solvents, which in turn prevent determination of the contrast matching point (see below). therefore, we assumed that the same difference in scattering length density exists between the carbon matrix and the interior of a pore on the one hand, and between the matrix and the solvent-accessible (macroscopic) extra particle void space on the other hand, and used the value of $\Delta\rho$ obtained from contrast matching at much lower Q, 0.01 $Å^{-1}$. Using this procedure we find for oxidized EA1 a density of spherical pores $n = 3.8 \times 10^{20}$ pores/cm^3 or a pore volume fraction of about 20%. For unoxidized EB1 the Guinier slope is the same indicating similar R_g but the volume fraction of pores calculated from the $Q = 0$ intercept is only 7%. While the absolute values for the volume fraction of the pores are approximate, we can be quiet confident in the relative difference in porosity between the two samples. We also estimated the fraction of graphene flakes arranged as isolated layers (i.e. with no interlayer correlations) using the R parameter introduced by Dahn's group [5], defined as the ratio of the (002) x-ray reflection intensity to the diffuse background. The (002) reflections are shown in Fig. 3, from which we deduce $R = 2.4$ and 11 for EA1 and EB1 respectively.

These values indicate a much higher degree of parallel (or nearly parallel) layers in the non-oxidized carbon. Coupled with the SANS results, the porosity appears to correlate with the isolated layer fraction.

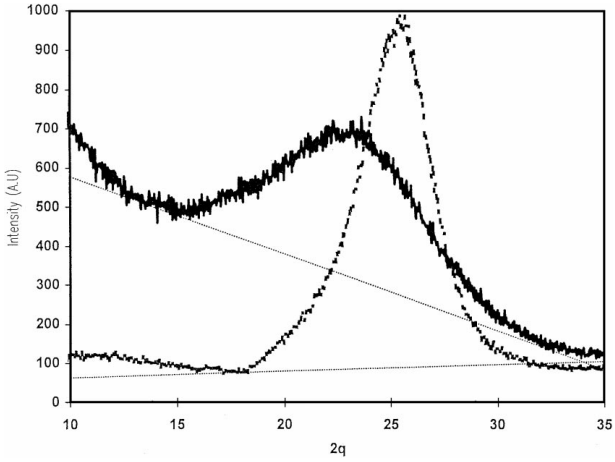

Figure 3 X-ray diffraction showing the "(002)" peak of EA1 (solid line) and EB1 (dased line); the dotted lines are the respective background scattering.

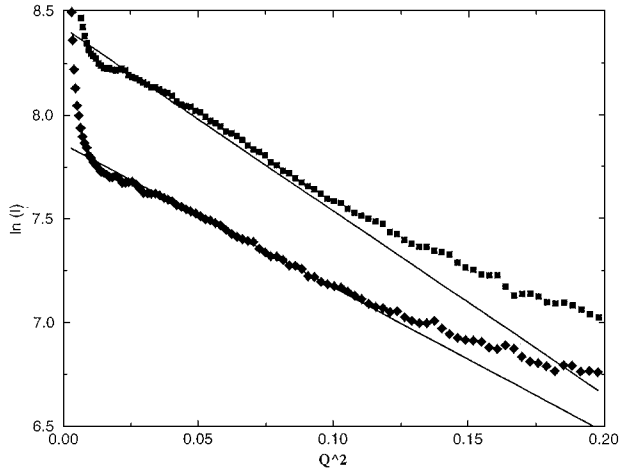

Figure 4 Guinier plot of pristine (squares) and doped (diamonds) ENR carbon. The lines are the linear fits.

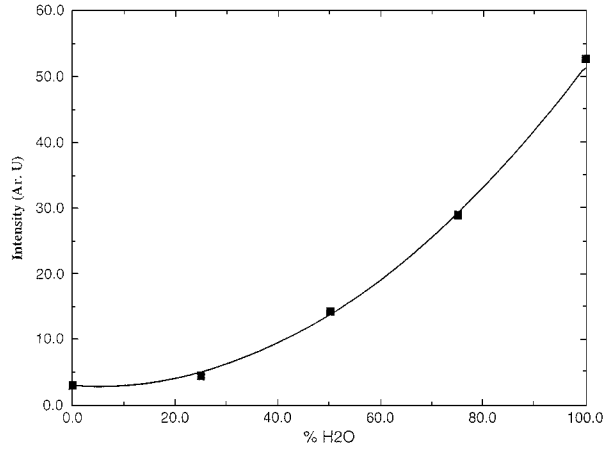

Figure 5 Contrast variation showing the SANS intensity at $Q = 0.01$ Å^{-1} from EA1 as a function of H_2O in a mixture of light and heavy water. Squares are the data and solid curve is a parabolic fit.

Previous structural study using radial distribution function analysis [6] revealed that such pitch-derived carbons consist of microscopic graphene fragments as small as 10 Å by 10 Å. Random stacking of such fragments would generate porosity on the order of 10 Å.

3.2. Effect of Li doping

Li insertion into EA1 has a significant effect on the high-Q scattering, as shown in Fig. 1 (circles). The scattering intensity is actually reduced compared to the pristine material. If Li clusters filled the vacuum pores, we would expect stronger scattering because the thermal neutron scattering length of Li is negative, and therefore filling the pores should increase the contrast ($\Delta\rho$ in Equation 2). The reduction in SANS intensity therefore suggests that Li does not fill vacuum pores, but rather "decorates" the pore surfaces (possibly attaching to dangling bonds created in the oxidation process) so that the contrast detected by the neutron lies between the average scattering length of the composite pore surface and the included vacuum. The pore radius in the doped sample is ∼4.5 Å, slightly less than the 5 Å in pristine sample, suggesting that the pore surfaces play a role in Li binding. A similar effect was also found in the ENR1000 carbon, the scattering from the pores decreases upon doping and the pores radius decrease as well as shown in Fig. 4. We determined that Li doping has no effect on the *R* parameter as measured from XRD.

3.3. Contrast variation

We performed contrast variation experiments by mixing EA1 with H_2O-D_2O solutions containing 100\%, 75\%, 50\%, 25\% and 0\% H_2O. The idea is to vary the density contrast between the inter-particle spaces and the bulk carbon and monitor the scattering intensity.

The scattering intensity at $Q = 0.01$ Å^{-1} as a function of H_2O fraction is presented in Fig. 5. The contrast matching point (the minimum) is found to occur at 7\% H_2O. This matching point is typical of carbons with low H content. We can conclude that the hydrogen is not concentrated on the particle's surface but equally distributed on the bulk. At higher *Q* the contrast effect is not as pronounced and the contrast matching condition shifts to higher H_2O content, indicating that water molecules do not permeate all the pores, which in turn is consistent with Swiss cheese structure of isolated pores. We did observe, however, some changes depending on solvent composition, which means that some pores are indeed vacuum and are solvent accessible. The contrast variation technique cannot provide unambiguous results if the scatterers are not accessible to the solvent [7].

4. Discussion

The structure of sp^2 hybridized disordered carbons is believed to consist of poly-hexagonal planar units (flakes, or "cards") whose size can be evaluated from the radial distribution function derived fromneutron diffraction experiments [6]. Using that technique a "card" consisting of 20–30 hexagons, roughly 10 Å × 10 Å, was found to be the building block of many "amorphous" carbons [6]. The excess Li capacity (beyond LiC_6) of such carbons is attributed to the possibility

of introducing two Li layers per carbon flake, or card, compared to one Li layer per carbon layer when the two layers are organized parallel to each other and separated by the crystallographic layer interval. On the other hand, since the hydrogen content of such carbons is insufficient to saturate the large density of edge carbons implied by small isolated "cards", and furthermore the ESR intensity (a measure of unsaturated edge carbons) is typically very low [8], a natural assumption is that the "cards" are not truly isolated but rather connected at the edges to form a wavy "potato-chip" structure [9]. One can imagine two different extreme scenarios for organizing such "chips" into a bulk solid, shown very schematically in Fig. 6. Two potato-chips could be staggered in the lateral direction (layers 1 and 2 in Fig. 6a) to form pores with R_g of order half the extent of a flat region, consistent with $R_g \sim 5$ Å from SANS and lateral dimension of flat chip segment 10 Å from RDF. In the other extreme, the the planar poly-hexagonal units are parallel (layers 2 and 3 in Fig. 6a), yielding no pores but a non-zero contribution to (002) pseudo-Bragg diffraction. (We have found by simulations [9] that, while perfectly parallel arrangement is unlikely in the real material, slightly tilted chip planes will still produce an "(002)" peak in x-ray diffraction). In this scenario, the Li capacity will increase as the fraction of potato-chips arranged "peak-to-peak", i.e. the pore-forming arrangement of layers 1 and 2, increases. Movement of some chips to the"peak-to-valley" configuration, which is energetically stabilized by the van der Waals interactions, would increase the (002) intensity (or *R* factor) and reduce the SANS intensity, without affecting the the average pore size. This effect could even be enhanced if we assume that the cards can change their bond angles upon heat treatment, in order to increase the van der Waals bonding with other layers. Thus the notion of "surfing cards", which would also decrease the Li capacity by reducing the fraction of chip segments available for two-sided Li doping.

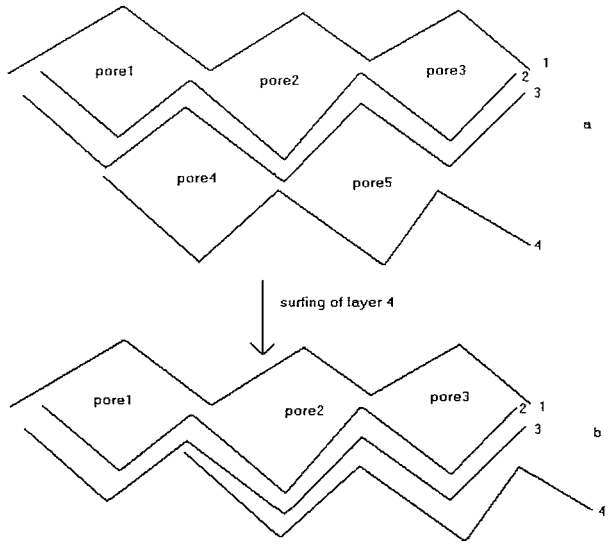

Figure 6 Schematic representation of the "surfing cards" model which attempts to explain changes in morphology and material performance with oxidation treatment. Before heat treatment (a) we see five pores and a single-layer fraction of 50\%, while after heat treatment (b) a single "layer" has "surfed" with respect to the others such that 2 of 5 pores are removed and the single-layer fraction is reduced to 25\% yielding a higher *R* value and lower Li capacity.

The above model, while highly schematic, correctly accounts for all the observed differences between oxidized and non-oxidized samples. One can speculate that oxygen atoms are preferentially bonded to the less stable carbons on the bending line between two planar units, thus increasing the energy barrier to potato-chip surfing. Recently, J. R. Dahn [10, 11] proposed a mechanism based on the "house of cards" model to account for the changes in porosity, (002) peak intensity and Li capacity upon heat treatment. Their "falling cards" model envisions the rotation of a single "card" into a parallel alignment with another card, thereby collapsing one small pore and creating a larger one, roughly doubling in R_g. This in turn reduces the single layer fraction (and hence Li capacity) and increases the (002) intensity and average pore radius. While this model appears to explain changes induced in many materials (e.g. sugars) with burn-off rate, it clearly cannot be applied to the coal pitch-derived carbons studied here. We found no change in pore size with oxidation, and the assumption of isolated single "cards" is not consistent with the low spin density and H content.

5. Conclusions

In this work we have demonstrated a correlation between microscopic density variations and Li capacity in oxidized disordered carbons. The reversible capacity increases with increasing porosity, an effect which is most likely due to an increase in the number of Li binding sites with oxidation and is certainly not associated with Li cluster formation inside the pores. Oxidation also reduces the fraction of parallel (or nearly parallel) graphene fragments, which in the "house of cards" model would imply a enhanced Li capacity. The results are qualitatively consistent with a "potato-chips" model of edge-connected "cards", which "surf" with respect to each other during thermal and oxidation treatments. Further work is clearly needed to elucidate the detailed microscopic processes involved in the oxidation treatment, while the present results provide a possibly better framework for approaching the problem.

Acknowledgements

We are grateful to the staff of the Cold Neutron Research Facility at NIST, in particular Tania Slaweki and William. A. Kamitakahara, for assistance with and introduction to the SANS technique. Research supported by Mitsubishi Chemical Company and Hughes Electronics Corp.

References

1. J. R. DAHN, T. ZHENG, Y. LIU and J. S. XUE, *Science* **270** (1995) 590.
2. K. TAKEI, N. TERADA, K. KUMAI, T. IWAHORI, T. UWAI and T. MIURA, *J. Power Sources* **55** (1995) 191.
3. B. HAMMOUDA, S. KRUEGER and C. J. GLINKA, *J. Res. NIST* **98** (1993) 31 .
4. L. A. FEIGIN and D. I. SVERGUN, "Structure Analysis by Small-Angle X-ray and Neutron Scattering" (Plenum, NY, 1987).

5. Y. LIU, J. S. XUE, T. ZHENG and J. R. DAHN, *Carbon* **34** (1996) 193.
6. P. ZHOU, P. PAPANEK, R. LEE, J. E. FISCHER and W. A. KAMIKATAHARA, *J. Electrochem. Soc.* **144** (1997) 1744.
7. M. A. FLORIANO, A. M. VENEZIA, G. DEGANELLO, E. C. SVENSSON and J. H. ROOT, *J. Appl. Cryst.* **27** (1994) 271.
8. K. TANAKA, T. KOIKE, T. YAMABE, J. YAMAUCHI, Y. DEGUCHI and S. YATA, *Phys. Rev. B* **15** (1987) 8368.
9. P. ZHOU, R. S. LEE, A. CLAYE and J. E. FISCHER, *Carbon* **36** (1998) 1777.
10. W. XING, J. S. XUE, T. ZHANG, A. GIBAUD and J. R. DAHN, *J. Electrochem. Soc.* **143** (1996) 3482.
11. J. R. DAHN, W. XING and Y. GAO, *Carbon* **35** (1997) 1997.

Received 29 July 1999
and accepted 10 February 2000